

# Mesoporous ZSM-5 Zeolite-Supported Ru Nanoparticles as Highly Efficient Catalysts for Upgrading Phenolic Biomolecules

Liang Wang,<sup>\*,†</sup> Jian Zhang,<sup>†</sup> Xianfeng Yi,<sup>‡</sup> Anmin Zheng,<sup>\*,‡</sup> Feng Deng,<sup>‡</sup> Chunyu Chen,<sup>†</sup> Yanyan Ji,<sup>†</sup> Fujian Liu,<sup>†</sup> Xiangju Meng,<sup>†</sup> and Feng-Shou Xiao<sup>\*,†</sup>

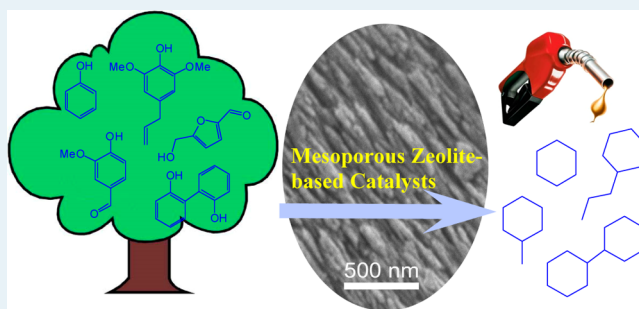
<sup>†</sup>Key Laboratory of Applied Chemistry of Zhejiang Province, Department of Chemistry, Zhejiang University, Hangzhou 310028, China

<sup>‡</sup>National Center for Magnetic Resonance in Wuhan, State Key Laboratory of Magnetic Resonance and Atomic and Molecular Physics and Mathematics, Wuhan Institute of Physics and Mathematics, Chinese Academy of Science, Wuhan 430071, China

## S Supporting Information

**ABSTRACT:** Zeolite-based catalysts have been widely used in the conversion of biomass recently, but the catalytic yields of the desired products are strongly limited by the relatively small micropores of zeolite. Here, we reported a hierarchically porous ZSM-5 zeolite with micropore and *b*-axis-aligned mesopore-supported Ru nanoparticles (Ru/HZSM-5-OM) that are highly efficient for the hydrodeoxygenation of both small and bulky phenolic biomolecules to the corresponding alkanes. Compared with the conventional ZSM-5 zeolite-supported Ru catalyst, the high catalytic activities and alkane selectivities over Ru/HZSM-5-OM are attributed to the abundant exposed acidic sites in HZSM-5-OM with open mesopores. This feature is potentially important for future phenolic bio-oil upgrading.

**KEYWORDS:** phenolic biomolecules, hydrodeoxygenation, mesoporous zeolite, Ru catalyst, biomass conversion



## 1. INTRODUCTION

Biomass, which is regarded as a renewable feedstock, has attracted attention for the production of fine chemicals and fuels.<sup>1–15</sup> Many economically viable processes have been developed for the conversion of biomass.<sup>1–5</sup> For example, fast pyrolysis of lignocellulosic biomass to produce phenolic bio-oil has been deemed a promising alternative to fossil fuels.<sup>16–24</sup> However, the direct use of phenolic bio-oils is impossible because their high oxygen content leads to low energy density, high viscosity, and low stability.<sup>16–19</sup> Therefore, upgrading bio-oils by hydrodeoxygenation is important to produce high-quality alkane bio-oils.

Recently, many Pd-, Ni-, and Pt-based catalysts have been reported to effectively catalyze the hydrodeoxygenation of the major components of phenolic bio-oils, such as phenol, syringol, furfural, and their derivatives.<sup>25–30</sup> To obtain high-quality alkanes, acids (e.g., phosphoric acid, acidic ionic liquids) mixed with metals are generally required for the cleavage of C–O bonds, which is a key step in the hydrodeoxygenation process. However, these homogeneous acids add complexity when regenerating the reaction systems, which is energy-consuming. More recently, as typical solid acids, aluminosilicate zeolites (e.g., ZSM-5, Beta) combined with metals have been employed to catalyze the hydrodeoxygenation of phenolic compounds to alkanes.<sup>7,25,26,31–33</sup> Because of the obvious advantages of high stability, easy separation, and abundant acidic sites, zeolite-based catalysts are regarded to be one of the most promising catalysts in the application of bio-oil upgrading. However, the

microporosity of the zeolite-based catalysts strongly limits the conversion of bulky biomolecules. Therefore, the production of relatively bulky bioalkanes is a challenge in the hydrodeoxygenation of phenolic bio-oil over zeolite-based catalysts.

Zeolites with hierarchical porous structures containing both micro- and mesopores, which are designated as mesoporous zeolites, have been developed.<sup>34–47</sup> The mesoporous zeolite-based catalysts have exhibited unique catalytic properties in many reactions compared with the conventional zeolites. For example, mesoporous ZSM-5 and Y zeolite-supported Pd and Pt–Pd metals are more active in hydrodesulfurization reactions than conventional zeolite-based catalysts.<sup>45,46</sup> The ZSM-5-based catalysts with mesopores gave much higher selectivity to C<sub>5</sub>–C<sub>11</sub> isoparaffins in Fischer–Tropsch reactions than the conventional ZSM-5-based catalyst.<sup>47</sup> However, catalytic conversion of biomass over the mesoporous zeolite-based catalysts is rarely reported, although the mesopores are favorable for the conversion of bulky biomass molecules. Herein, we show that the mesoporous ZSM-5 zeolite (ZSM-5-M)-supported Ru nanoparticles are efficient catalysts for the hydrodeoxygenation of the phenolic compounds in bio-oil to alkanes. Particularly, *b*-axis-aligned mesoporous ZSM-5 (ZSM-5-OM), a new type of mesoporous zeolite with *b*-axis-aligned mesopore-supported

Received: October 31, 2014

Revised: March 17, 2015

Published: March 17, 2015

Ru nanoparticles, are very active for the production of alkane bio-oils because of the open mesopores on ZSM-5-OM with rich exposed acid sites for catalyzing the cleavage of C–O bonds, a key step in the hydrodeoxygenation of phenolic molecules to alkanes.

## 2. EXPERIMENTAL SECTION

**2.1. Materials.** All reagents were of analytical grade and were used as purchased without further purification. Tetrapropyl ammonium hydroxide (TPAOH, 20.1 wt %),  $\text{CH}_3\text{I}$ , DMF, phenol, 5-hydroxymethylfurfural (HMF), glucose, 1-ethyl-3-methylimidazolium chloride, and 2,6-dimethoxyphenol were purchased from Aladdin Company. 4-Allyl-2-methoxyphenol, 4-allyl-2,6-dimethoxyphenol, 4-hydroxy-3-methoxybenzaldehyde, 4-ethyl-2-methoxyphenol, and biphenyl-2,2'-diol, 1-(4-hydroxyphenyl)-2-phenylethanone were purchased from Kaide Chemical Co. Tetraethyl orthosilicate (TEOS),  $\text{NaAlO}_2$ , petroleum ether, ammonium nitrate, and NaOH were purchased from Tianjin Guangfu Chemical Co. Cationic polydiallyldimethylammonium chloride (PDADMAC, 10 wt %, molecular weight approximately  $1.5 \times 10^5$ ) was purchased from Yinhu Chemical Co.  $\text{RuCl}_3$  was obtained from Huishui Tech. Co. Copolymer polystyrene-*co*-4-polyvinylpyridine (molecular weight approximately  $1.6 \times 10^5$ , PSt-*co*-P4VP) was obtained from Sigma-Aldrich Company. Quaternary ammoniation of PSt-*co*-P4VP by  $\text{CH}_3\text{I}$  to obtain C-PSt-*co*-P4VP was performed according to the literature.<sup>44</sup>

**2.2. Synthesis of ZSM-5 and ZSM-5-M.** In a typical synthesis of ZSM-5 zeolite, (1) 8 mL of tetrapropyl ammonium hydroxide (TPAOH, 19.4 wt %) and 93 mg of  $\text{NaAlO}_2$  were added to 20 mL of water. (2) Then, the mixture was stirred at room temperature for 2 h, and 7 mL of TEOS was added. (3) After stirring overnight, the gel was transferred into an autoclave to crystallize at 180 °C for 3 days. (4) By filtrating, drying, and calcining at 550 °C for 4 h, the ZSM-5 sample was obtained. The ZSM-5-M was synthesized under the same conditions except for the addition of 1.2 g of PDADMAC after the addition of TEOS. After ammonium anion exchange with ammonium nitrate and calcination, the H-form zeolite was obtained.

**2.3. Synthesis of ZSM-5-OM.** In a typical run, 0.08 g of  $\text{NaAlO}_2$ , 12.5 mL of TPAOH (20.1 wt %), and 7.0 mL of TEOS were mixed, followed by the addition of 20 mL of water. After stirring at room temperature for 6 h and aging at 100 °C for 2 h, a clear zeolite precursor was obtained. Meanwhile, 2 g of quaternary ammoniated polyvinylpyridine polymer (molecular weight approximately  $1.6 \times 10^5$ , C-PSt-*co*-P4VP) was dissolved into 5 mL of water, followed by the addition of 3 mL of TPAOH, giving a C-PSt-*co*-P4VP solution. After mixing the clear zeolite precursor with the C-PSt-*co*-P4VP solution, the mixture was stirred for 24 h at room temperature, then transferred into an autoclave for crystallization at 180 °C for 3.5 days. After filtration, drying, calcination at 550 °C in oxygen, ammonium anion exchange with ammonium nitrate, and calcination again, the H-form zeolite was obtained.

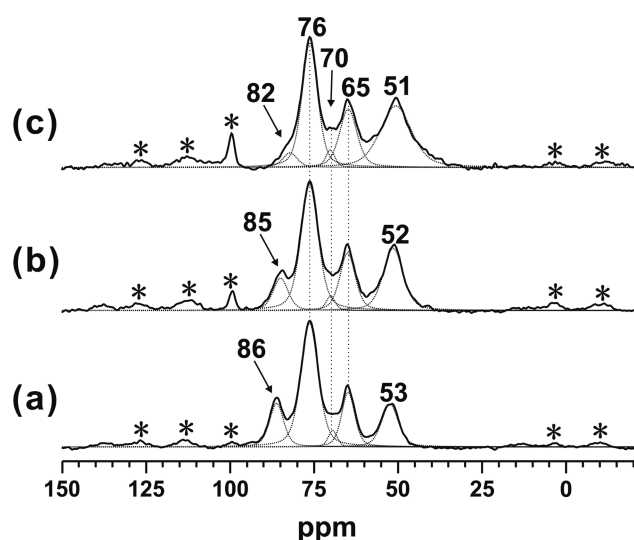
**2.4. Synthesis of Ru/HZSM-5, Ru/HZSM-5-M, Ru/HZSM-5-OM, Pt/HZSM-5, Pd/HZSM-5, and Ru/NaZSM-5.** In a typical run, 1 g of the solid support (e.g., HZSM-5) was stirred in 50 mL of  $\text{RuCl}_3$  solution with the desired Ru concentration for 12 h, followed by evaporating the excess water at 80 °C, heating at 100 °C for 12 h, and washing with a large amount of water. Then, the solid powder was calcined in air at 400 °C for 2 h and was reduced by  $\text{H}_2$  at 250 °C for 2 h to obtain the final samples.

**2.5. Synthesis of Ru/SBA-15, Ru/ $\text{Al}_2\text{O}_3$ , and Au/ZSM-5.** In a typical run, 1 g of the solid support (e.g., SBA-15) was

added to 50 mL of  $\text{RuCl}_3$  solution with the desired Ru concentration. After adding urea (molar ratio of urea/Ru of 100) and stirring at 90 °C for 4 h in a closed reactor kept away from light, the solid sample was filtrated, washed with a large amount of water, dried at 100 °C for 12 h, calcined at 400 °C for 3 h, and reduced by  $\text{H}_2$  at 250 °C for 2 h to obtain the final samples.

**2.6. Characterization.** Powder X-ray diffraction patterns (XRD) were obtained with a Rigaku powder X-ray diffractometer using  $\text{CuK}\alpha$  radiation ( $\lambda = 0.1542$  nm). X-ray photoelectron spectroscopy (XPS) was performed on a Thermo ESCALAB 250 with  $\text{Al K}\alpha$  radiation at  $\theta = 90^\circ$  for the X-ray source. The binding energies were calibrated using the C 1s peak at 285.0 eV. The metal content was determined by inductively coupled plasma spectroscopy (ICP, PerkinElmer 3300DV). Nitrogen sorption isotherms were measured at  $-196$  °C using a Micromeritics ASAP 2020 M system. The samples were degassed for 10 h at 150 °C before the measurements. The mesopore size distributions were determined using the Barrett–Joyner–Halenda (BJH) model. Scanning electron microscopy (SEM) was performed using a Hitachi SU 1510. Transmission electron microscope (TEM) images were collected using a Hitachi HT-7700. NMR experiments were performed on a Bruker Ascend-500 spectrometer at a resonance frequency of 202.63 MHz for  $^{31}\text{P}$ , with a 4 mm triple-resonance MAS probe at a spinning rate of 10 kHz.  $^{31}\text{P}$  MAS NMR spectra with high power proton decoupling were recorded using a  $\pi/2$  pulse length of 4.1  $\mu\text{s}$  and a recycle delay of 30 s. The chemical shift of  $^{31}\text{P}$  was referenced to 1 M aqueous  $\text{H}_3\text{PO}_4$ . Prior to the adsorption of the probe molecules, the acid samples were placed in glass tubes and connected to a vacuum line for dehydration. The temperature was gradually increased at a rate of 1 °C  $\text{min}^{-1}$ , and the samples were kept at a final temperature of 400 °C and a pressure below  $10^{-3}$  Pa over a period of 10 h and were then cooled. After the samples cooled to ambient temperature, a known amount of trimethylphosphine oxide (TMPO) was introduced into the acid. The activated samples were frozen by liquid  $\text{N}_2$ , followed by elimination of the physisorbed probe molecules by evacuation at room temperature for 10 min. Finally, the sample tubes were flame-sealed. The preparation of the TMPO adsorbed sample was performed according to the method proposed by our previous work.<sup>49</sup> Prior to the NMR experiments, the sealed samples were transferred into  $\text{ZrO}_2$  rotors with a Kel-F end-cap under a dry nitrogen atmosphere in a glovebox.

**2.7. Catalytic Tests.** The hydrodeoxygenation was performed in a high-pressure autoclave with a magnetic stirrer (1200 rpm). Typically, the substrate, catalyst, and solvent were mixed in the reactor by stirring for 10 min at room temperature. Then, hydrogen was introduced and maintained at the desired pressure, and the reaction system was heated to a given temperature (the temperature was measured with a thermometer in an oil bath, and the hydrogen pressure in the autoclave was recorded at the reaction temperature). After the reaction, the product was removed from the reaction system and analyzed by gas chromatography (GC-14C, Shimadzu, using a flame ionization detector) with a flexible quartz capillary column coated with OV-17 and FFAP and a high-pressure liquid chromatograph (HPLC1200, Agilent) equipped with a Ca cation exchange column and methanol (0.4 mL/min) as the eluent. The substrate conversions and product selectivities are based on the carbon atoms in the molecules using ethylbenzene as the internal standard. The recyclability of the catalyst was



**Figure 1.**  $^{31}\text{P}$  NMR spectra of TMPO adsorbed on (a) HZSM-5, (b) HZSM-5-M, and (c) HZSM-5-OM. The asterisks in the  $^{31}\text{P}$  NMR spectra denote spinning sidebands due to the strong interactions between TMPO and the Brønsted acid sites.

**Table 1. Measurement Data for the  $^{31}\text{P}$  NMR of TMPO Adsorbed on HZSM-5, HZSM-5-M, and HZSM-5-OM**

| samples    | $^{31}\text{P}$ NMR peak/ppm relative concentration (%) |      |     |      |       |
|------------|---|------|-----|------|-------|
|            | 51–53   | 65   | 70  | 76   | 82–86 |
| H-ZSM-5    | 16.4  | 16.5 | 3.4 | 49.5 | 14.3  |
| H-ZSM-5-M  | 25.0  | 18.0 | 2.7 | 44.5 | 9.9   |
| H-ZSM-5-OM | 36.5  | 19.3 | 3.1 | 37.1 | 4.1   |

tested by separating it from the reaction system by centrifugation, washing it with a large quantity of ethanol and drying it at 100 °C for 4 h.

The conversion of glucose to 5-hydroxymethylfurfural (HMF) was performed in a 25 mL glass reactor with a magnetic stirrer in an oil bath. In a typical run, glucose and [Emim] Cl (1-ethyl-3-methylimidazolium chloride) were mixed in the reactor and stirred (1200 rpm) at the reaction temperature for

10 min (the temperature was measured with a thermometer in the oil bath). Then, the catalyst was added to the reaction mixture. After the reaction, the HMF product was analyzed by gas chromatography (GC-14C) with a flexible quartz capillary column (OV-17) using ethylbenzene as an internal standard.

### 3. RESULT AND DISCUSSION

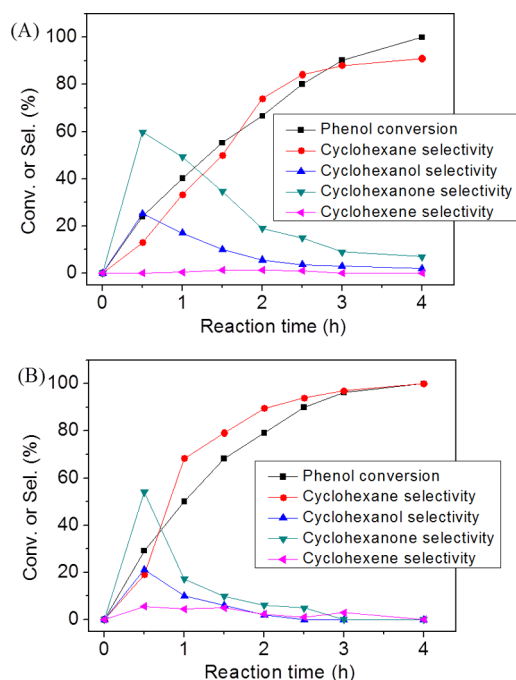
**3.1. Synthesis and Characterization.** The ZSM-5-OM sample (Si/Al = 42) was synthesized according to the reported literature, using tetrapropyl ammonium hydroxide and copolymer polystyrene-*co*-4-polyvinylpyridine as templates.<sup>44</sup> After calcination to remove the organic template and ion-exchange treatment, the H-form ZSM-5-OM zeolite (HZSM-5-OM) was obtained (Figure S1–S3). Then, the Ru nanoparticles were loaded on the HZSM-5-OM support by the impregnation method (Ru/HZSM-5-OM, Figure S4–S8). The Ru content in Ru/HZSM-5-OM was 1.1 wt %, as analyzed by inductively coupled plasma (ICP). For comparison, the conventional ZSM-5 zeolite (Ru/HZSM-5) and mesoporous ZSM-5 zeolite-supported Ru catalyst (Ru/HZSM-5-M) was also prepared (Figure S4–S8). The textural parameters of various samples are listed in Table S1.

Figure 1 shows the  $^{31}\text{P}$  NMR spectra of trimethylphosphine oxide (TMPO) adsorbed on various samples, which is a unique and practical technique to characterize the acid strength and host/guest interaction in solid acid catalysts.<sup>48,49</sup> On the basis of our previous work, the confinement effect of the zeolite framework is important in determining the  $^{31}\text{P}$  chemical shift of TMPO adsorbed on the Brønsted acid sites.<sup>49,50</sup> The channel diameter of ZSM-5 is approximately 0.55–0.60 nm, which is comparable to the molecular size of TMPO with a kinetic diameter of 0.55 nm. The more complete pore structure inside ZSM-5 facilitates the investigation of the long-range electrostatic effects from the Madelung potential of the zeolite framework (confinement effect), which is pronounced for the microporous channels of ZSM-5 zeolite.<sup>50</sup> Thus, the  $^{31}\text{P}$  chemical shift can be used to characterize the integrity of the zeolite micropores. As shown in Figure 1, the HZSM-5, HZSM-5-M, and HZSM-5-OM samples give five signals at 51–53, 65, 70, 76, and 82–86 ppm, associated with TMPO adsorbed at the

**Table 2. Catalytic Data for the Hydrodeoxygenation of Phenol and 2,6-Dimethoxyphenol over Various Catalysts<sup>a</sup>**

| entry | substrate           | catalyst                          | conv (%) | product selectivity (%) <sup>b</sup> |              |                     | carbon balance (%) |
|-------|---------------------|-----------------------------------|----------|--------------------------------------|--------------|---------------------|--------------------|
|       |                     |                                   |          | cyclohexane                          | cyclohexanol | cyclohexanone       |                    |
| 1     | phenol              | Ru/HZSM-5                         | >99.5    | 91.0                                 | 2.0          | 7.0                 | >99.5              |
| 2     | phenol              | Pt/HZSM-5                         | >99.5    | 55.0                                 | 29.0         | 16.0                | >99.5              |
| 3     | phenol              | Pd/HZSM-5                         | >99.5    | 88.4                                 | 11.6         |                     | >99.5              |
| 4     | phenol              | Ni/HZSM-5                         | 42.2     | 40.0                                 | 15.5         | 44.5                | >99.5              |
| 5     | phenol              | Au/HZSM-5                         | <1.0     |                                      |              |                     | >99.5              |
| 6     | phenol              | Ru/NaZSM-5                        | 98.1     |                                      | 99.0         | 1.0                 | >99.5              |
| 7     | phenol              | Ru/Al <sub>2</sub> O <sub>3</sub> | >99.5    |                                      | 90.0         | 10.0                | >99.5              |
| 8     | phenol              | Ru/SBA-15                         | 89.9     |                                      | 94.0         | 6.0                 | >99.5              |
| 9     | phenol              | Ru/HZSM-5-M                       | >99.5    | 95.4                                 | 4.0          | 0.6                 | >99.5              |
| 10    | phenol              | Ru/HZSM-5-OM                      | >99.5    | 95.0                                 | 5.0          | 0.9                 | >99.5              |
|       |                     |                                   |          | cyclohexane                          | methanol     | others <sup>c</sup> |                    |
| 11    | 2,6-dimethoxyphenol | Ru/HZSM-5                         | 70.0     | 55.4                                 | 17.0         | 15.0                | 93.2 <sup>d</sup>  |
| 12    | 2,6-dimethoxyphenol | Ru/HZSM-5-M                       | 81.0     | 57.7                                 | 16.9         | 6.9                 | 91.0 <sup>d</sup>  |
| 13    | 2,6-dimethoxyphenol | Ru/HZSM-5-OM                      | 97.5     | 70.0                                 | 19.7         | 2.0                 | 92.4 <sup>d</sup>  |

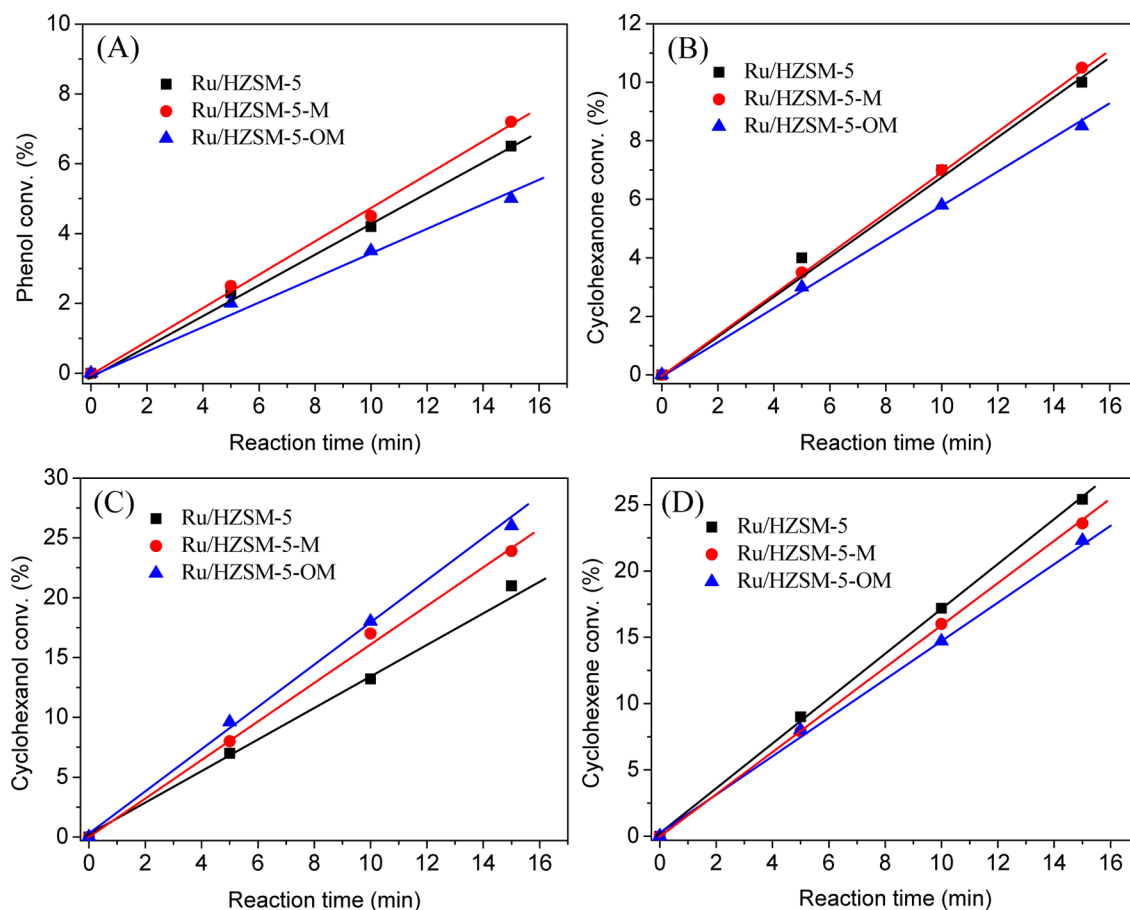
<sup>a</sup>Reaction conditions: 150 °C, 4 h, 4.0 MPa of H<sub>2</sub>, 50 mg of catalyst, 1 mmol of phenolic substrate, 8 mL of water. <sup>b</sup>(C atoms in each product/total C atoms in all products) × 100%. <sup>c</sup>Cyclohexanol- and cyclohexanone-derived molecules and some others. <sup>d</sup>The undetected carbon was mainly due to the volatilization of the methanol product.



**Figure 2.** Dependences of phenol conversion and product selectivity on time over (A) Ru/HZSM-5 and (B) Ru/HZSM-5-OM catalysts. The reaction conditions are the same to those in Table 2.

different acid sites on the varied zeolites. Notably, the  $^{31}\text{P}$  chemical shift is at 86 ppm in HZSM-5 and is attributed to the  $\text{Al}_{12}-\text{O}_{24}-\text{Si}_{12}$  site in ZSM-5 zeolite with a 10-membered ring (10MR) structure<sup>49</sup> was shifted slightly to 85 ppm over the HZSM-5-M and significantly to 82 ppm over HZSM-OM. This significant  $^{31}\text{P}$  chemical shift toward the high-field indicates that the host/guest interactions are decreased by the presence of open mesopores in H-ZSM-5-OM. Furthermore, the quantitative amount of each acid site can be obtained from the  $^{31}\text{P}$  peak intensity. As listed in Table 1, the relative amount of  $^{31}\text{P}$  peak at 82–86 ppm is dramatically decreased from 14.3% (HZSM-5) to 9.9% (HZSM-5-M) and 4.1% (HZSM-5-OM). Meanwhile, the  $^{31}\text{P}$  peak at approximately 50 ppm, assigned to TMPO adsorbed in the mesopores and/or on the external acid sites, significantly increased in intensity from 16.4% (HZSM-5) to 25.0% (HZSM-5-M) and 36.5% (HZSM-5-OM), indicating that the HZSM-5-OM has significantly more exposed acidic sites in the open mesopores. This feature is favorable for the catalytic conversion of bulky molecules, such as bulky biomass molecules. In addition, these samples exhibited similar peaks at 76, 70, and 65 ppm, which are ascribed to TMPO adsorbed on the acidic protons located at different T sites with different acid strengths in H-ZSM-5 zeolite.<sup>50</sup>

**3.2. Hydrodeoxygenation of Phenol.** Table 2 shows the catalytic data for the hydrodeoxygenation of the relatively small molecule of phenol and the bulky molecule of 2,6-dimethoxyphenol



**Figure 3.** Dependences of substrate conversion on time over Ru/HZSM-5, Ru/HZSM-5-M, and Ru/HZSM-5-OM catalysts in (A) hydrogenation of phenol, (B) hydrogenation of cyclohexanone, (C) dehydration of cyclohexanol, (D) hydrogenation of cyclohexene. Reaction conditions: 150 °C, 4.0 MP of  $\text{H}_2$  ( $\text{N}_2$  was used in the dehydration reaction), 30 mg of catalyst, 1 mmol of phenolic substrate, 8 mL of water. The hydrogen was introduced into the reactor after the required temperature was achieved.

Table 3. Reaction Rates of Various Catalysts in Different Reactions

| entry | reactions                         | reaction rate (mmol g <sup>-1</sup> h <sup>-1</sup> ) |             |              |
|-------|-----------------------------------|---|-------------|--------------|
|       |                                   | Ru/HZSM-5   | Ru/HZSM-5-M | Ru/HZSM-5-OM |
| 1     | phenol hydrogenation              | 8.5   | 8.8         | 6.2          |
| 2     | cyclohexanone hydrogenation       | 13.3  | 14.0        | 10.7         |
| 3     | cyclohexanol dehydration          | 28.0  | 31.8        | 34.6         |
| 4     | cyclohexene hydrogenation         | 33.9  | 31.5        | 29.7         |
| 5     | 2,6-dimethoxyphenol hydrogenation | 6.9   | 7.2         | 6.0          |
| 6     | 2-methoxycyclohexanol dehydration | 0.4   | 2.0         | 4.4          |

as the model phenolic molecules of bio-oils. Typically, in the hydrodeoxygenation of phenol to cyclohexane, cyclohexanone, cyclohexanol, and cyclohexene are formed as intermediates (Scheme S1, Figure 2). The Ru/HZSM-5, Pd/HZSM-5, and Pt/HZSM-5 catalysts are catalytically active, with phenol conversion higher than 99.5% (entries 1–3 in Table 2). In addition, Ru/HZSM-5 shows higher cyclohexane selectivity (91.0%) than Pt/HZSM-5 and Pd/HZSM-5 (55.0–88.4%). These results suggest that Ru/HZSM-5 is suitable for the hydrodeoxygenation of phenol.

The Na-form of ZSM-5 zeolite-supported Ru nanoparticles (Ru/NaZSM-5) gave cyclohexanol as a major product with a selectivity of 99.0% (entry 6 in Table 2). Similarly, the Ru/Al<sub>2</sub>O<sub>3</sub> and Ru/SBA-15 catalysts have cyclohexanol as a major product (selectivities at 90.0–94.0%, entries 7 and 8 in Table 2). This phenomenon is attributed to the absence of Brønsted acid sites on NaZSM-5, Al<sub>2</sub>O<sub>3</sub>, and SBA-15 supports, which are inactive for the dehydration of cyclohexanol, an important step during the hydrodeoxygenation of phenol to cyclohexane (Scheme S1). Ru/HZSM-5, Ru/HZSM-5-M, and Ru/HZSM-5-OM catalysts have similar conversion (>99.5%) and cyclohexane selectivities (91.0–95.4%) in phenol hydrodeoxygenation (entries 1, 9, and 10 in Table 2). To understand their activities, Figure 3 shows the dependences of substrate conversion on time over these catalysts in the elementary reactions of phenol dehydroxylation, including hydrogenation of phenol, hydrogenation of cyclohexanone, dehydration of cyclohexanol, and hydrogenation of cyclohexene (Scheme S1). Based on the fitted straight line, the reaction rates of each catalyst are calculated and are presented in Table 3.

The reaction rates are in the following: *phenol hydrogenation* < *cyclohexanone hydrogenation* < *cyclohexanol dehydration* < *cyclohexene hydrogenation*. These results indicate that the hydrogenation of phenol is a control step for the overall reaction rate of phenol hydrodeoxygenation. Because Ru/HZSM-5, Ru/HZSM-5-M, and Ru/HZSM-5-OM catalysts have similar reaction rates in phenol hydrogenation (6.2–8.8 mmol g<sup>-1</sup> h<sup>-1</sup>, Table 3), it is reasonable that the three catalysts have similar conversion and selectivity in phenol hydrodeoxygenation.

### 3.3. Hydrodeoxygenation of 2,6-Dimethoxyphenol.

Ru/HZSM-5-M, Ru/HZSM-5-OM, and Ru/HZSM-5 catalysts exhibit distinguishable catalytic performance in the hydrodeoxygenation of bulky 2,6-dimethoxyphenol (Tables 2 and S2). For example, Ru/HZSM-5-OM has a cyclohexane selectivity of 70.0% (entry 13 in Table 2), whereas Ru/HZSM-5 has a selectivity of 55.4% (entry 11 in Table 2). In this reaction, the dehydration step (dehydration of 2-methoxycyclohexanol) is the control step, giving reaction rates of 0.4–4.4 mmol g<sup>-1</sup> h<sup>-1</sup> (Table 3). Therefore, the high yield of cyclohexane product in the hydrodeoxygenation of 2,6-dimethoxyphenol over Ru/HZSM-5-OM is attributed to its higher rate (4.4 mmol g<sup>-1</sup> h<sup>-1</sup>) in the 2-methoxycyclohexanol dehydration step than

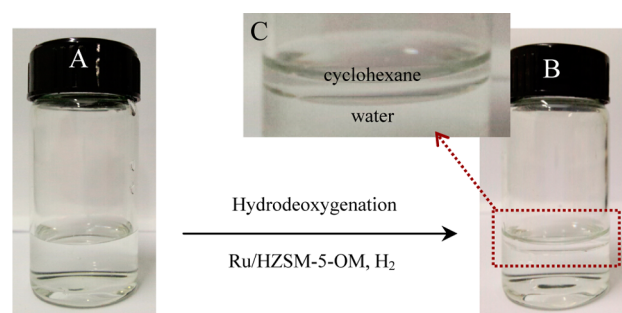


Figure 4. Photographs of the reaction mixture of 2,6-dimethoxyphenol in water (A) before and (B) after the 5-g scale hydrodeoxygenation over Ru/HZSM-5-OM catalyst. (C) Enlarged photograph showing the phase separation of cyclohexane from water.

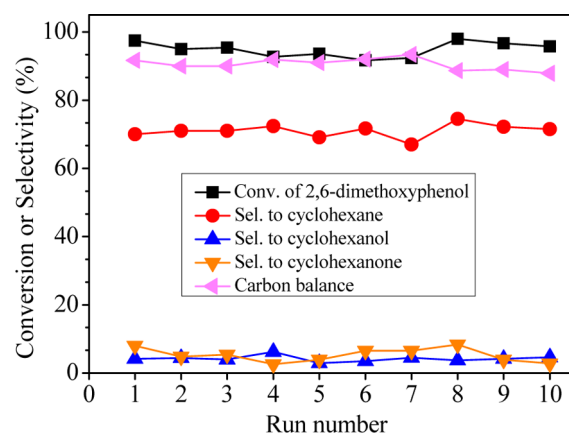


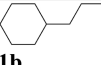
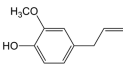

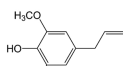
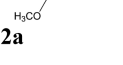

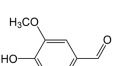
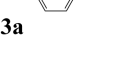
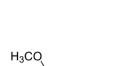
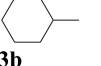
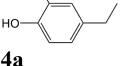
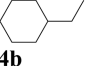

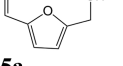

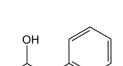
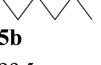
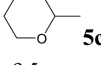
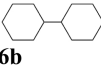
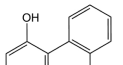
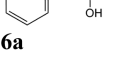


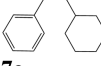
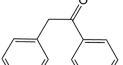
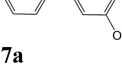
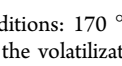
Figure 5. Recycling tests of Ru/HZSM-5-OM in the hydrodeoxygenation of 2,6-dimethoxyphenol. The reaction conditions are the same as those in Table 1. The catalyst was calcined at 480 °C for 4 h before the 8th use.

that over Ru/HZSM-5 and Ru/HZSM-5-M (0.4–2.0 mmol g<sup>-1</sup> h<sup>-1</sup>).

Because the bulky 2,6-dimethoxyphenol molecule could not transfer through the small micropores of ZSM-5 zeolite, the dehydration of 2,6-dimethoxyphenol occurs on the external/mesopore acid sites of the ZSM-5-based catalysts.<sup>35–46</sup> Therefore, the different activities of the Ru/HZSM-5, Ru/HZSM-5-M, and Ru/HZSM-5-OM catalysts in the 2,6-dimethoxyphenol dehydration are attributed to the differences in the accessible acidic sites of 2,6-dimethoxyphenol on the zeolite catalysts. The Ru/HZSM-5-OM has more accessible acidic sites in the mesopores for the 2,6-dimethoxyphenol molecules than Ru/HZSM-5, in good agreement with the observations from the <sup>31</sup>P MAS NMR technique (Figures 1, S9, and S10, Tables 1, S1, S3, and S4).

Based on these observations, it is proposed that the significantly better catalytic properties in the hydrodeoxygenation

Table 4. Catalytic Hydrodeoxygenation of Various Phenolic Monomers and Dimers over Various Catalysts<sup>a</sup>

| Entry | Reactant  | Catalyst   | Conv. (%) | Product selectivity (%)   |                     |              |                     | Carbon Balance (%) <sup>b</sup> |
|-------|---|--|-----------|---|---------------------|--------------|---------------------|---------------------------------|
|       |   |  |           | <br><b>1b</b>    | cyclohexane         | cyclohexanol | cyclohexanone       |                                 |
| 1     |    | Ru/HZSM-5-OM                                       | >99.5     | 83.0  | --                  | 6.9          | 2.2                 | 91.4                            |
| 2     |    | Ru/HZSM-5-M  | 97.0      | 80.4  | --                  | 6.0          | 6.0                 | 92.6                            |
| 3     |    | Ru/HZSM-5  | 77.4      | 49.2  | 4.4                 | 5.0          | 38.0                | 97.4                            |
| 4     |    | Pd/C + H <sub>3</sub> PO <sub>4</sub> <sup>f</sup> | 99.0      | 65.0  | 8.5                 | 7.4          | 18.0                |                                 |
| 5     |    | Ru/HZSM-5-OM                                       | 98.4      | 70.0  | --                  | 14.2         | 6.2                 | 90.6                            |
| 6     |    | Ru/HZSM-5-M  | 75.9      | 72.9  | --                  | 15.0         | 7.6                 | 96.6                            |
| 7     |    | Ru/HZSM-5  | 61.4      | 37.9  | 1.0                 | 10.9         | 42.6                | 95.3                            |
| 8     |    | Pd/C + H <sub>3</sub> PO <sub>4</sub> <sup>f</sup> | 92.0      | 58.0  | 9.0                 | 12.0         | 21.0                |                                 |
|       |   |  |           | <br><b>3b</b>    | Isomeric alkanes    | Methanol     | Others <sup>d</sup> |                                 |
| 9     |    | Ru/HZSM-5-OM                                       | >99.5     | 84.0  | --                  | 6.0          | 1.0                 | 91.0                            |
|       |   |  |           | <br><b>4b</b>    | Isomeric alkanes    | Methanol     | Others <sup>d</sup> |                                 |
| 10    |   | Ru/HZSM-5-OM                                       | >99.5     | 85.2  | --                  | 7.7          | 1.1                 | 94.0                            |
| 11    |  | Ru/HZSM-5-OM                                       | >99.5     | 90.5  | 9.5                 |              |                     | >99.5                           |
| 12    |  | Ru/HZSM-5-M  | >99.5     | 74.2  | 25.8                |              |                     | >99.5                           |
| 13    |  | Ru/HZSM-5  | >99.5     | 69.0  | 31.0                |              |                     | >99.5                           |
|       |   |  |           | <br><b>5b</b>   |                     |              |                     |                                 |
|       |   |  |           | <br><b>5c</b>  |                     |              |                     |                                 |
|       |   |  |           | <br><b>6b</b>  | Others <sup>d</sup> |              |                     |                                 |
| 14    |  | Ru/HZSM-5-OM                                       | >99.5     | 81.4  | 18.6                |              |                     | >99.5                           |
| 15    |  | Ru/HZSM-5-M  | >99.5     | 52.2  | 47.8                |              |                     | >99.5                           |
| 16    |  | Ru/HZSM-5  | 97.0      | 44.7  | 55.3                |              |                     | >99.5                           |
|       |   |  |           | <br><b>7b</b>  |                     |              |                     |                                 |
|       |   |  |           | <br><b>7c</b> |                     |              |                     |                                 |
| 17    |  | Ru/HZSM-5-OM                                       | >99.5     | 62.4  | 30.0                | 7.6          |                     | 98.0                            |
| 18    |  | Ru/HZSM-5-M  | >99.5     | 37.7  | 52.0                | 10.3         |                     | 99.1                            |
| 19    |  | Ru/HZSM-5  | 92.0      | 12.4  | 87.0                | 0.6          |                     | 99.0                            |

<sup>a</sup>Reaction conditions: 170 °C, 4 h, 4.0 MP of H<sub>2</sub>, 50 mg of catalyst, 1 mmol of phenolic substrate, 8 mL of water. <sup>b</sup>The undetected carbon was mainly due to the volatilization of methanol product. <sup>c</sup>The data were obtained from ref 7. <sup>d</sup>Cyclic alcohols, ketones, aromatics, and some others.

of 2,6-dimethoxyphenol over Ru/HZSM-5-OM than over Ru/HZSM-5-M and Ru/HZSM-5 result from the presence of *b*-axis-aligned mesopores in the ZSM-5 crystals, which improve the access of bulky molecules to the acidic sites in the zeolite catalysts.

A series of solvents, such as water, methanol, ethanol, ethyl acetate, and dodecane, were employed in the dehydration of phenol, and water was a suitable solvent in this reaction (Table S5). After hydrodeoxygenation in water solvent, the water-soluble phenolic molecules were transformed into the water insoluble alkanes, where the phase separation of alkanes from the water solvent promoted the shift of the reaction balance to the formation of alkanes (Figure 4). Because the

production of phenolic molecules from biomass is always performed with water, the use of water solvent in this reaction has advantages, such as high efficiency, low cost, and easy separation of the cyclohexane product.<sup>51</sup> Furthermore, we performed the 2,6-dimethoxyphenol hydrodeoxygenation on a 5-g scale in water solvent over Ru/HZSM-5-OM catalyst. In this case, high 2,6-dimethoxyphenol conversion (94.4%) and good cyclohexane selectivity (71.4%) were obtained. The phase separation of the cyclohexane product from water solvent was obvious (Figure 4C).

Figure 5 shows the recycling tests of Ru/HZSM-5-OM catalyst in the hydrodeoxygenation of 2,6-dimethoxyphenol. After recycling ten times, Ru/HZSM-5-OM still gives high

2,6-dimethoxyphenol conversion (95.8%) and good cyclohexane selectivity (69.0%), which are similar to those (97.5 and 70.0%) of the as-synthesized Ru/HZSM-5-OM. These results confirm the excellent recyclability of the Ru/HZSM-5-OM catalyst. At the same time, the Ru species in the liquid collected from the reaction mixture is undetectable by ICP analysis, indicating that metal leaching is almost negligible under the reaction conditions.

**3.4. Hydrodeoxygenation of Various Phenolic Monomers and Dimers.** Table 4 shows the catalytic data for the Ru catalysts in the hydrodeoxygenation of various biofuel-derived phenolic monomers and dimers to produce C<sub>6</sub>–C<sub>14</sub> alkanes. The various Ru catalysts are active with alkanes, aromatics, cycloalcohols, cycloketones, and methanol as products at reaction temperature of 170 °C. For example, in the hydrodeoxygenation of **1a**, Ru/HZSM-5-OM gives a full conversion of **1a** with selectivity to **1b** at 83.0% (entry 1 in Table 4). In contrast, Ru/HZSM-5 exhibits lower **1a** conversion (77.4%) and **1b** selectivity (49.2%, entry 3 in Table 4). The combined Pd/C and phosphoric acid catalyst, one of the most active catalysts for hydrodeoxygenation reported previously, exhibits **1a** conversion at 99.0% and **1b** selectivity at 65.0% at relatively high temperature (250 °C, entry 4 in Table 4).<sup>7</sup>

Furthermore, Ru/HZSM-5-OM has much higher activity and C<sub>9</sub> alkane selectivity in the hydrodeoxygenation of **2a** than Ru/HZSM-5-M and Ru/HZSM-5 catalysts. Particularly, Ru/HZSM-5-OM has higher activity and selectivity than the combined Pd/C and phosphoric acid catalyst (entries 5 and 8 in Table 4). When substrates **3a** and **4a** are used, Ru/HZSM-5-OM is also very active (entries 9 and 10 in Table 4). When 5-hydroxymethylfurfural (HMF, **5a**) is chosen as a substrate, Ru/HZSM-5-OM has much higher product selectivity than Ru/HZSM-5-M and Ru/HZSM-5 (entries 11–13 in Table 4). In addition to the phenolic monomers, we also compared the catalytic performance in the hydrodeoxygenation of phenolic dimers of **6a** and **7a** over the catalysts. Ru/HZSM-5-OM shows significantly higher C<sub>12</sub> and C<sub>14</sub> alkane selectivities for **6b** and **7b** (81.4 and 62.4%, entries 14 and 17 in Table 4) than Ru/HZSM-5-M (52.2 and 37.7%, entries 15 and 18 in Table 4) and Ru/HZSM-5 (44.7 and 12.4%, entries 16 and 19 in Table 4). These results demonstrate the excellent catalytic properties of Ru/HZSM-5-OM in the hydrodeoxygenation of bio-oil molecules.

**3.5. Conversion of Glucose to HMF.** It is interesting to note that the concept of mesopore zeolite-based catalysts for biomass conversion is not limited to hydrodeoxygenation but can be applied to the production of platform chemicals, such as HMF. For example, in the conversion of glucose to the platform molecule HMF, HZSM-5-OM exhibits more excellent catalytic properties than the HZSM-5-M and HZSM-5 catalysts (Figure S11). The further details are still under investigation.

## 4. CONCLUSIONS

In summary, we report that the *b*-axis aligned mesoporous zeolite-supported Ru catalyst (Ru/HZSM-5-OM) exhibits high catalytic activities, excellent selectivity, and extraordinary stability for upgrading phenolic bio-oils into alkanes. The excellent catalytic properties of Ru/HZSM-5-OM are strongly related to the open mesopores of HZSM-5-OM, which has accessible acidic sites exposed to bulky molecules. Considering most biomass molecules in nature are much larger than the micropore sizes of zeolites, mesoporous zeolites are an alternative route for efficient conversion of the biomass to biofuels and biochemicals in the future.

## ■ ASSOCIATED CONTENT

### Supporting Information

The following file is available free of charge on the ACS Publications website at DOI: 10.1021/acscatal.5b00083.

TEM, XPS, XRD, and SEM characterizations and catalytic data (PDF)

## ■ AUTHOR INFORMATION

### Corresponding Authors

\*E-mail: liangwang@zju.edu.cn (L.W.).

\*E-mail: zhenganm@wipm.ac.cn (A.Z.).

\*E-mail: fsxiao@zju.edu.cn (F.-S.X.).

### Notes

The authors declare no competing financial interest.

## ■ ACKNOWLEDGMENTS

This work is supported by the National Natural Science Foundation of China (21333009, 21403192, and 21403193), the National High-Tech Research and Development program of China (2013AA065301), and the China Postdoctoral Science Foundation (2014M550318).

## ■ REFERENCES

- (1) Corma, A.; Iborra, S.; Velty, A. *Chem. Rev.* **2007**, *107*, 2411–2502.
- (2) Do, P. T. M.; McAtee, J. R.; Watson, D. A.; Lobo, R. F. *ACS Catal.* **2013**, *3*, 41–46.
- (3) Tessonier, J. P.; Villa, A.; Majoulet, O.; Su, D. S.; Schlogl, R. *Angew. Chem., Int. Ed.* **2009**, *48*, 6543–6546.
- (4) Wan, X.; Zhou, C.; Chen, J.; Deng, W.; Zhang, Q.; Yang, Y.; Wang, Y. *ACS Catal.* **2014**, *4*, 2175–2185.
- (5) Choudhary, V.; Pinar, A. B.; Sandler, S. I.; Vlachos, D. G.; Lobo, R. F. *ACS Catal.* **2011**, *1*, 1724–1728.
- (6) Roman-Leshkov, Y.; Barrett, C. J.; Liu, Z. Y.; Dumesic, J. A. *Nature* **2007**, *447*, 982–986.
- (7) Zhao, C.; Kou, Y.; Lemonidou, A. A.; Li, X.; Lercher, J. A. *Angew. Chem., Int. Ed.* **2009**, *48*, 3987–3990.
- (8) Wang, L.; Xiao, F.-S. *Green Chem.* **2015**, *17*, 24–39.
- (9) Bi, Q.-Y.; Du, X.-L.; Liu, Y.-M.; Cao, Y.; He, H.-Y.; Fan, K.-N. *J. Am. Chem. Soc.* **2012**, *134*, 8926–8933.
- (10) Wang, L.; Wang, H.; Liu, F.; Zhang, A.; Zhang, J.; Sun, Q.; Lewis, J. P.; Zhu, L.; Meng, X.; Xiao, F.-S. *ChemSusChem* **2014**, *7*, 402–406.
- (11) Lam, E.; Luong, J. H. T. *ACS Catal.* **2014**, *4*, 3393–3410.
- (12) Román-Leshkov, Y.; Moliner, M.; Labinger, J. A.; Davis, M. E. *Angew. Chem., Int. Ed.* **2010**, *49*, 8954–8957.
- (13) Yang, J.; Li, N.; Li, S.; Wang, W.; Li, L.; Wang, A.; Wang, X.; Cong, Y.; Zhang, T. *Green Chem.* **2014**, *16*, 4879–4884.
- (14) Li, J.; Liu, L.; Liu, Y.; Li, M.; Zhu, Y.; Liu, H. C.; Kou, Y.; Zhang, J.; Han, Y.; Ma, D. *Energy Environ. Sci.* **2014**, *7*, 393–398.
- (15) Luo, C.; Wang, S. A.; Liu, H. C. *Angew. Chem., Int. Ed.* **2007**, *46*, 7636–7639.
- (16) Liu, D. J.; Chen, E. Y.-X. *ACS Catal.* **2014**, *4*, 1302–1310.
- (17) Mohan, D.; Pittman, C. U.; Steele, P. H. *Energy Fuels* **2006**, *20*, 848–889.
- (18) Xia, Q.-N.; Cuan, Q.; Liu, X.-H.; Gong, X.-Q.; Lu, G.-Z.; Wang, Y.-Q. *Angew. Chem., Int. Ed.* **2014**, *53*, 9755–9760.
- (19) Liu, S.-S.; Sun, K.-Q.; Xu, B.-Q. *ACS Catal.* **2014**, *4*, 2226–2230.
- (20) Huber, G. W.; Corma, A. *Angew. Chem., Int. Ed.* **2007**, *46*, 7184–7201.
- (21) Wang, H. M.; Male, J.; Wang, Y. *ACS Catal.* **2013**, *3*, 1047–1070.
- (22) Peng, B.; Yao, Y.; Zhao, C.; Lercher, J. A. *Angew. Chem., Int. Ed.* **2012**, *51*, 2072–2075.

- (23) Peng, B.; Yuan, X.; Zhao, C.; Lercher, J. A. *J. Am. Chem. Soc.* **2012**, *134*, 9400–9405.
- (24) Wang, L.; Zhang, B.; Meng, X.; Su, D. S.; Xiao, F.-S. *ChemSusChem* **2014**, *7*, 1537–1541.
- (25) Zhao, C.; Lercher, J. A. *Angew. Chem., Int. Ed.* **2012**, *51*, 5935–5940.
- (26) Hong, D.-Y.; Miller, S. J.; Agrawal, P. K.; Jones, C. W. *Chem. Commun.* **2010**, *46*, 1038–1040.
- (27) Ohta, H.; Kobayashi, H.; Hara, K.; Fukuoka, A. *Chem. Commun.* **2011**, *47*, 12209–12211.
- (28) Sergeev, A. G.; Hartwig, J. F. *Science* **2011**, *332*, 439–443.
- (29) Echeandia, S.; Arias, P. L.; Barrio, V. L.; Pawelec, B.; Fierro, J. L. G. *Appl. Catal., B* **2010**, *101*, 1–12.
- (30) Yan, N.; Yuan, Y.; Dykeman, R.; Kou, Y.; Dyson, P. J. *Angew. Chem., Int. Ed.* **2010**, *49*, 5549–5553.
- (31) Zhao, C.; Camaioni, D. M.; Lercher, J. A. *J. Catal.* **2012**, *288*, 92–103.
- (32) Zhang, W.; Chen, J.; Liu, R.; Wang, S.; Chen, L.; Li, K. *ACS Sustainable Chem. Eng.* **2014**, *2*, 683–691.
- (33) Zhu, X. L.; Lobban, L. L.; Mallinson, R. G.; Resasco, D. E. *J. Catal.* **2011**, *281*, 21–29.
- (34) Zhang, X. Y.; Liu, D. X.; Xu, D. D.; Asahina, S.; Cychosz, K. A.; Agrawal, K. V.; Al Wahedi, Y.; Bhan, A.; Al Hashimi, S.; Terasaki, O.; Thommes, M.; Tsapatsis, M. *Science* **2012**, *336*, 1684–1687.
- (35) Sun, Y. Y.; Prins, R. *Angew. Chem., Int. Ed.* **2008**, *47*, 8478–8481.
- (36) Neumann, G. T.; Hicks, J. C. *ACS Catal.* **2012**, *2*, 642–646.
- (37) Yoo, W. C.; Kumar, S.; Penn, R. L.; Tsapatsis, M.; Stein, A. J. *Am. Chem. Soc.* **2009**, *131*, 12377–12383.
- (38) Zhu, K.; Sun, J.; Liu, J.; Wang, L.; Wan, H.; Hu, J.; Wang, Y.; Peden, C. H. F.; Nie, Z. *ACS Catal.* **2011**, *1*, 682–690.
- (39) Choi, M.; Cho, H. S.; Srivastava, R.; Venkatesan, C.; Choi, D. H.; Ryoo, R. *Nat. Mater.* **2006**, *5*, 718–723.
- (40) Choi, M.; Na, K.; Kim, J.; Sakamoto, Y.; Terasaki, O.; Ryoo, R. *Nature* **2009**, *461*, 246–249.
- (41) Zou, X.; Conradsson, T.; Klingstedt, M.; Dadachov, M. S.; O’Keeffe, M. *Nature* **2005**, *437*, 716–719.
- (42) Xiao, F.-S.; Wang, L. F.; Yin, C. Y.; Lin, K. F.; Di, Y.; Li, J.; Xu, R.; Su, D. S.; Schlogl, R.; Yokoi, T.; Tatsumi, T. *Angew. Chem., Int. Ed.* **2006**, *45*, 3090–3093.
- (43) Zhu, J.; Zhu, Y.; Zhu, L.; Rigutto, M.; van der Made, A.; Yang, C.; Pan, S.; Wang, L.; Zhu, L.; Jin, Y.; Sun, Q.; Wu, Q.; Meng, X.; Zhang, D.; Han, Y.; Li, J.; Chu, Y.; Zheng, A.; Qiu, S.; Zheng, X.; Xiao, F.-S. *J. Am. Chem. Soc.* **2014**, *136*, 2503–2510.
- (44) Liu, F.; Willhammar, T.; Wang, L.; Zhu, L.; Sun, Q.; Meng, X.; Carrillo-Cabrera, W.; Zou, X.; Xiao, F.-S. *J. Am. Chem. Soc.* **2012**, *134*, 4557–4560.
- (45) Tang, T.; Zhang, L.; Fu, W.; Ma, Y.; Xu, J.; Jiang, J.; Fang, G.; Xiao, F.-S. *J. Am. Chem. Soc.* **2013**, *135*, 11437–11440.
- (46) Fu, W.; Zhang, L.; Tang, T.; Ke, Q.; Wang, S.; Hu, J.; Fang, G.; Li, J.; Xiao, F.-S. *J. Am. Chem. Soc.* **2011**, *133*, 15346–15349.
- (47) Kang, J.; Cheng, K.; Zhang, L.; Zhang, Q.; Ding, J.; Hua, W.; Lou, Y.; Zhai, Q.; Wang, Y. *Angew. Chem., Int. Ed.* **2011**, *50*, 5200.
- (48) Karra, M. D.; Sutovich, K. J.; Mueller, K. T. *J. Am. Chem. Soc.* **2002**, *124*, 902–903.
- (49) Zheng, A. M.; Huang, S.-J.; Liu, S.-B.; Deng, F. *Phys. Chem. Chem. Phys.* **2011**, *13*, 14889–14901.
- (50) Zheng, A. M.; Zhang, H. L.; Lu, X.; Liu, S. B.; Deng, F. *J. Phys. Chem. B* **2008**, *112*, 4496–4505.
- (51) He, J.; Zhao, C.; Lercher, J. A. *J. Catal.* **2014**, *309*, 362–375.